Chapter 7
Periodic Response Prediction for Hybrid and Piecewise Linear Systems

G. Manson

Abstract This chapter presents a completely novel framework for the prediction and understanding of nonlinear system behavior. The idea is simply that all nonlinear systems can be represented as a combination of linear systems between which information is exchanged. Under harmonic excitation, the periodic responses of such hybrid systems may be easily calculated when the switching between linear systems is specified in terms of time. These time-switching hybrid systems provide a useful stepping stone to more realistic piecewise linear systems where the switching criteria are specified in terms of displacement and/or velocity. This chapter details the framework and illustrates its ability to efficiently predict the periodic responses from piecewise linear systems. The framework is also shown to be capable of predicting both stable and unstable periodic responses for conditions where jump behavior is possible. The extension of the work to continuous nonlinear systems is also briefly discussed.

Keywords Nonlinear · Hybrid systems · Piecewise linear

7.1 Introduction

The environmental and economic pressures of the last couple of decades have resulted in an unprecedented effort on the part of structural design engineers to design structures that are more lightweight than, yet are at least as strong as, their structural ancestors. While this drive for strong, lightweight structures is clearly desirable, in many cases, this will also result in the structural response becoming significantly nonlinear. While research has been conducted into nonlinear system behavior for centuries, the current situation appears to be, as Worden and Tomlinson wrote in their monograph "Nonlinearity in Structural Dynamics" [1] that "there is no unique approach to dealing with the problem of nonlinearity either analytically or experimentally and thus we must be prepared to experiment with several approaches." The primary aim of this monograph was to introduce and explain a number of these approaches that would belong in a "toolbox" for the analysis of nonlinear structural systems and included Harmonic Balance [2], Hilbert Transform [3], NARMAX modeling [4], the Masri-Caughey Restoring Force Surface method [5], Direct Parameter Estimation [6], and the Volterra Series approximation [7]. Approaches not considered in the monograph included perturbation methods [8], multiple scales [9], and nonlinear normal modes [10]. The research conducted using the aforementioned approaches over the last five or so decades has undoubtedly led to much greater understanding of the behavior of nonlinear systems and has resulted in countless applications. That said, it is fair to say that all approaches are not without their limitations. These limitations are often associated with the need for approximation or, where infinite series are being employed, are associated with the related issues of series convergence and truncation. Another limitation with the bulk of these approaches is that they are only capable of representing what is often termed "weak nonlinearity."

One of the reasons as to why there has not yet emerged a General Theory of Nonlinearity may be in the nonlinear dynamicists' simple system of choice, namely, the Duffing oscillator [11]. While the classical Duffing oscillator model of a linear plus cubic stiffness term lends itself as a good approximation for many real engineering systems, it may not have been the best starting point for the development of a General Theory. The author would instead like to propose that a better starting point may be provided via hybrid systems and, their close counterparts, piecewise linear systems. The reason behind this proposal is that the responses of such systems may be written in terms of linear steady-state and linear transient

G. Manson (✉)
Dynamics Research Group, Department of Mechanical Engineering, University of Sheffield, Sheffield, UK
e-mail: graeme.manson@sheffield.ac.uk

M. R. W. Brake et al. (eds.), *Nonlinear Structures & Systems, Volume 1*, Conference Proceedings
of the Society for Experimental Mechanics Series, https://doi.org/10.1007/978-3-031-36999-5_7

components without any recourse to a framework that presupposes the nature of the resulting response. Within the field of Control Engineering, hybrid systems are very well known and there have been several papers [12–14] that have demonstrated that such systems are capable of the most extreme form of nonlinear behavior, namely, chaos. It should be stated however that these papers all relied upon numerical simulation as opposed to any theoretical framework, which is the purpose of this chapter.

The layout of this chapter is as follows: Sect. 7.2 develops the closed-form solution for the periodic response of a harmonically-excited time-switched hybrid system. Section 7.3 introduces an iterative approach that allows the closed-form solution of the previous section to be used for the prediction of periodic responses of piecewise linear systems, including the identification of stable and unstable solutions when the jump phenomenon is present. Section 7.4 rounds off with some discussion including how the approach may eventually be extended to predict the periodic responses of the Duffing oscillator.

7.2 Periodic Response of Harmonically-Excited Time-Switched Hybrid Systems

In this section, the format of the hybrid system will be introduced, followed by the development of the theory regarding the calculation of the periodic responses of these systems. The hybrid system will be composed of n linear systems with a single linear system being active at any point in time. The equation of motion for the ith linear system is written in nondimensional form:

$$\ddot{Y}(\tau) + \underbrace{2\zeta_i \left(\dot{Y}(\tau) - \dot{Y}_{\text{offset}_i}\right)}_{F_{\text{d}_i}} + \underbrace{\gamma_i \left(Y(\tau) - Y_{\text{offset}_i}\right)}_{F_{\text{s}_i}} = \cos(\alpha\tau) \tag{7.1}$$

The above equation allows each linear system to have individual damping and stiffness parameters ζ_i and γ_i. The inclusion of $\dot{Y}_{\text{offset}_i}$ and Y_{offset_i} means that the zero values of damping force F_{d_i} and stiffness force F_{s_i} may occur at nonzero values of velocity and displacement, respectively.

The time point at which the active system changes will be referred to as a time switch. There will be multiple time switches and therefore, there will be multiple response segments. Assuming that the jth response segment occurs when the ith linear system is active, the total output displacement and velocity response segments, $Y_j(\tau)$ and $\dot{Y}_j(\tau)$, respectively, may be expressed as a sum of the steady-state and transient response segments:

$$\begin{aligned} Y_j(\tau) &= Y_{\text{ss}_j}(\tau) + Y_{\text{tr}_j}(\tau) \\ \dot{Y}_j(\tau) &= \dot{Y}_{\text{ss}_j}(\tau) + \dot{Y}_{\text{tr}_j}(\tau) \end{aligned} \tag{7.2}$$

The steady-state displacement response segment $Y_{\text{ss}_j}(\tau)$ may be written as follows:

$$Y_{\text{ss}_j}(\tau) = \frac{2\zeta_i}{\gamma_i}\dot{Y}_{\text{offset}_i} + Y_{\text{offset}_i} + |H_i(\alpha)| \cos\left(\alpha\tau + \angle H_i(\alpha)\right) \tag{7.3}$$

where $H_i(\alpha)$, the frequency response function (FRF) of the ith linear system, is given by

$$H_i(\alpha) = \frac{1}{\gamma_i - \alpha^2 + i2\zeta_i\alpha} \tag{7.4}$$

The steady-state velocity response segment $\dot{Y}_{\text{ss}_j}(\tau)$ is the derivative of Eq. (7.3):

$$\dot{Y}_{\text{ss}_j}(\tau) = -\alpha\,|H_i(\alpha)| \sin\left(\alpha\tau + \angle H_i(\alpha)\right) \tag{7.5}$$

The transient displacement response segment $Y_{\text{tr}_j}(\tau)$ will be written as follows:

$$Y_{\text{tr}_j}(\tau) = \exp\left(-\zeta_i\left(\Delta\tau_j\right)\right)\left[A_j \cos\left(\beta_i\left(\Delta\tau_j\right)\right) + B_j \sin\left(\beta_i\left(\Delta\tau_j\right)\right)\right] \tag{7.6}$$

where $\beta_i = \sqrt{\gamma_i - \zeta_i^2}$ and $\Delta\tau_j$ is the dimensionless time measured from the point at which the system became active. The transient parameters A_j and B_j will be calculated to ensure that the displacement and velocity values of the newly active system and those of the previously active system are the same at the point of switching.

The transient velocity response segment $\dot{Y}_{\mathrm{tr}_j}(\tau)$ is the derivative of Eq. (7.6):

$$\dot{Y}_{\mathrm{tr}_j}(\tau) = \exp\left(-\zeta_i\left(\Delta\tau_j\right)\right)\left[\left(\beta_i B_j - \zeta_i A_j\right)\cos\left(\beta_i\left(\Delta\tau_j\right)\right) + \left(-\beta_i A_j - \zeta_i B_j\right)\sin\left(\beta_i\left(\Delta\tau_j\right)\right)\right] \tag{7.7}$$

The above equations may now be used for the first idea of this chapter, namely, that the periodic response of harmonically-excited hybrid systems, subjected to time switches that occur at the same point in the forcing cycle, may be expressed in a closed-form. It is assumed that the system parameters will be specified for each system as will the forcing frequency ratio α. Information regarding the times at which specific linear systems become active will also need to be specified. If there are a total of m time switches, vectors of size $1 \times m$ must be specified that state which linear system becomes active at each switch and the time at which that switch occurs. The active system vector will be labeled S and the time switch vector will be labeled τ_{sw}. All elements S_j (where $j = 1, \ldots, m$) must be integers between 1 and n, while all elements τ_{sw_j} (where $j = 1, \ldots, m$) must be between zero and the repeat period $\tau_{\mathrm{period}} = 2\pi/\alpha$. It is also necessary that successive elements of τ_{sw} must increase in value (in order to give a positive value for time spent in each active system) – there can be a single decrease in value, which will describe a "wrap-around" effect into the next forcing period. This concept should become clearer when an illustrative example is considered shortly. Once the τ_{sw} vector has been specified, the $\Delta\tau$ vector that details the time spent in each active system segment may be calculated.

The time spent in system S_j (if $j \neq m$) is given by

$$\begin{aligned} \Delta\tau_j &= \tau_{\mathrm{sw}_{j+1}} - \tau_{\mathrm{sw}_j} \text{ if } \tau_{\mathrm{sw}_{j+1}} > \tau_{\mathrm{sw}_j} \\ \Delta\tau_j &= \tau_{\mathrm{period}} + \tau_{\mathrm{sw}_{j+1}} - \tau_{\mathrm{sw}_j} \text{ if } \tau_{\mathrm{sw}_{j+1}} < \tau_{\mathrm{sw}_j} \end{aligned} \tag{7.8}$$

and, if $j = m$, the time spent in system S_j is given by

$$\begin{aligned} \Delta\tau_j &= \tau_{\mathrm{sw}_1} - \tau_{\mathrm{sw}_m} \text{ if } \tau_{\mathrm{sw}_1} > \tau_{\mathrm{sw}_m} \\ \Delta\tau_j &= \tau_{\mathrm{period}} + \tau_{\mathrm{sw}_1} - \tau_{\mathrm{sw}_m} \text{ if } \tau_{\mathrm{sw}_1} < \tau_{\mathrm{sw}_m} \end{aligned} \tag{7.9}$$

As stated previously, the closed-form expression for the periodic responses of harmonically-excited hybrid systems will be derived via equating the displacement of the newly active system to that of the previously active system at each time switch and doing the same with the velocity. Expressing the displacements and velocities in terms of steady-state and transient components gives rise to expressions that equate the steady-state differences to the transient differences as shown below (for $j \neq 1$):

$$\begin{aligned} Y_{\mathrm{tr}_j}\left(\tau_{\mathrm{sw}_j}\right) - Y_{\mathrm{tr}_{j-1}}\left(\tau_{\mathrm{sw}_j}\right) &= Y_{\mathrm{ss}_{j-1}}\left(\tau_{\mathrm{sw}_j}\right) - Y_{\mathrm{ss}_j}\left(\tau_{\mathrm{sw}_j}\right) \\ \dot{Y}_{\mathrm{tr}_j}\left(\tau_{\mathrm{sw}_j}\right) - \dot{Y}_{\mathrm{tr}_{j-1}}\left(\tau_{\mathrm{sw}_j}\right) &= \dot{Y}_{\mathrm{ss}_{j-1}}\left(\tau_{\mathrm{sw}_j}\right) - \dot{Y}_{\mathrm{ss}_j}\left(\tau_{\mathrm{sw}_j}\right) \end{aligned} \tag{7.10}$$

and, for $j = 1$,

$$\begin{aligned} Y_{\mathrm{tr}_1}\left(\tau_{\mathrm{sw}_1}\right) - Y_{\mathrm{tr}_m}\left(\tau_{\mathrm{sw}_1}\right) &= Y_{\mathrm{ss}_m}\left(\tau_{\mathrm{sw}_1}\right) - Y_{\mathrm{ss}_1}\left(\tau_{\mathrm{sw}_1}\right) \\ \dot{Y}_{\mathrm{tr}_1}\left(\tau_{\mathrm{sw}_1}\right) - \dot{Y}_{\mathrm{tr}_m}\left(\tau_{\mathrm{sw}_1}\right) &= \dot{Y}_{\mathrm{ss}_m}\left(\tau_{\mathrm{sw}_1}\right) - \dot{Y}_{\mathrm{ss}_1}\left(\tau_{\mathrm{sw}_1}\right) \end{aligned} \tag{7.11}$$

The steady-state displacement for the jth response segment (i.e., when system S_j is active) at the kth time switch is given by

$$Y_{\mathrm{ss}_j}\left(\tau_{\mathrm{sw}_k}\right) = \frac{2\zeta_{\mathrm{S}_j}}{\gamma_{S_j}}\dot{Y}_{\mathrm{offset}_{S_j}} + Y_{\mathrm{offset}_{S_j}} + \left|H_{S_j}(\alpha)\right|\cos\left(\alpha\tau_{\mathrm{sw}_k} + \angle H_{S_j}(\alpha)\right) \tag{7.12}$$

and the corresponding steady-state velocity is

$$\dot{Y}_{\mathrm{ss}_j}\left(\tau_{\mathrm{sw}_k}\right) = -\alpha\left|H_{S_j}(\alpha)\right|\sin\left(\alpha\tau_{\mathrm{sw}_k} + \angle H_{S_j}(\alpha)\right) \tag{7.13}$$

The transient displacement and velocity expressions at each time switch are a little less straightforward, and it is also necessary to develop expressions that relate the transient behavior between successive time switches. The transient displacement for the *j*th response segment (i.e., when system S_j is active) is given by

$$Y_{\mathrm{tr}_j}\left(\tau_{\mathrm{sw}_j}+\tau_j\right)=\exp\left(-\zeta_{S_j}\tau_j\right)\left[A_j\cos\left(\beta_{S_j}\tau_j\right)+B_j\sin\left(\beta_{S_j}\tau_j\right)\right] \tag{7.14}$$

where τ_j varies from 0 (when system S_j becomes active) to $\Delta\tau_j$ (when system S_j stops being active). Similarly, the velocity response for the *j*th response segment is given by a slightly modified version of Eq. (7.16):

$$\dot{Y}_{\mathrm{tr}_j}\left(\tau_{\mathrm{sw}_j}+\tau_j\right)=\exp\left(-\zeta_{S_j}\tau_j\right)\left[\left(\beta_{S_j}B_j-\zeta_{S_j}A_j\right)\cos\left(\beta_{S_j}\tau_j\right)+\left(-\beta_{S_j}A_j-\zeta_{S_j}B_j\right)\sin\left(\beta_{S_j}\tau_j\right)\right] \tag{7.15}$$

Setting τ_j equal to zero in the above two expressions and rearranging a little gives expressions for the transient parameters A_j and B_j in terms of the transient displacement and velocity at the time switch where system S_j becomes active. Similarly, setting τ_j equal to $\Delta\tau_j$ in Eqs. (7.14) and (7.15) gives expressions for the transient displacement and velocity for system S_j at the time switch where it stops being active. These four equations may be combined to express the equality of the displacements and velocities of the previously active and newly active systems at any switch point. For τ_{sw_j}, the displacement and velocity equalities may be presented in matrix form:

$$\begin{bmatrix} \mathrm{ec}_{j-1}+\frac{\zeta_{S_{j-1}}}{\beta_{S_{j-1}}}\mathrm{es}_{j-1} & \frac{1}{\beta_{S_{j-1}}}\mathrm{es}_{j-1} & 1 & 0 \\ \frac{-\beta_{S_{j-1}}^2-\zeta_{S_{j-1}}^2}{\beta_{S_{j-1}}}\mathrm{es}_{j-1} & \mathrm{ec}_{j-1}-\frac{\zeta_{S_{j-1}}}{\beta_{S_{j-1}}}\mathrm{es}_{j-1} & 0 & 1 \end{bmatrix}\begin{Bmatrix} Y_{\mathrm{tr}_{j-1}}\left(\tau_{\mathrm{sw}_{j-1}}\right) \\ \dot{Y}_{\mathrm{tr}_{j-1}}\left(\tau_{\mathrm{sw}_{j-1}}\right) \\ Y_{\mathrm{tr}_j}\left(\tau_{\mathrm{sw}_j}\right) \\ \dot{Y}_{\mathrm{tr}_j}\left(\tau_{\mathrm{sw}_j}\right) \end{Bmatrix}=\begin{Bmatrix} Y_{\mathrm{ss}_{j-1}}\left(\tau_{\mathrm{sw}_j}\right)-Y_{\mathrm{ss}_j}\left(\tau_{\mathrm{sw}_j}\right) \\ \dot{Y}_{\mathrm{ss}_{j-1}}\left(\tau_{\mathrm{sw}_j}\right)-\dot{Y}_{\mathrm{ss}_j}\left(\tau_{\mathrm{sw}_j}\right) \end{Bmatrix} \tag{7.16}$$

where the shorthand notation ec_{j-1} represents $\exp\left(-\zeta_{S_{j-1}}\left(\Delta\tau_{j-1}\right)\right)\cos\left(\beta_{S_{j-1}}\left(\Delta\tau_{j-1}\right)\right)$ and es_{j-1} represents $\exp\left(-\zeta_{S_{j-1}}\left(\Delta\tau_{j-1}\right)\right)\sin\left(\beta_{S_{j-1}}\left(\Delta\tau_{j-1}\right)\right)$.

Repeating this for all m time switches results in the matrix expression $[\lambda]\{T\}=\{\phi\}$ where $[\lambda]$ is a $2m\times 2m$ matrix given by

$$[\lambda]=\begin{bmatrix} q_1 & r_1 & 1 & 0 & 0 & 0 & \cdots & 0 & 0 \\ s_1 & t_1 & 0 & 1 & 0 & 0 & \cdots & 0 & 0 \\ 0 & 0 & q_2 & r_2 & 1 & 0 & \cdots & 0 & 0 \\ 0 & 0 & s_2 & t_2 & 0 & 1 & \cdots & 0 & 0 \\ \vdots & \vdots & \vdots & \vdots & \vdots & \vdots & \ddots & \vdots & \vdots \\ 1 & 0 & 0 & 0 & 0 & 0 & \cdots & q_m & r_m \\ 0 & 1 & 0 & 0 & 0 & 0 & \cdots & s_m & t_m \end{bmatrix} \tag{7.17}$$

where

$$\begin{aligned} q_j &= \mathrm{ec}_j+\frac{\zeta_{S_j}}{\beta_{S_j}}\mathrm{es}_j, \quad & r_j &= \frac{1}{\beta_{S_j}}\mathrm{es}_j, \\ s_j &= \frac{-\beta_{S_j}^2-\zeta_{S_j}^2}{\beta_{S_j}}\mathrm{es}_j, \quad & t_j &= \mathrm{ec}_j-\frac{\zeta_{S_j}}{\beta_{S_j}}\mathrm{es}_j \end{aligned} \tag{7.18}$$

$\{T\}$ and $\{\phi\}$ are $2m\times 1$ column vectors given by

$$\{T\}=\begin{Bmatrix} Y_{\mathrm{tr}_1}\left(\tau_{\mathrm{sw}_1}\right) \\ \dot{Y}_{\mathrm{tr}_1}\left(\tau_{\mathrm{sw}_1}\right) \\ Y_{\mathrm{tr}_2}\left(\tau_{\mathrm{sw}_2}\right) \\ \dot{Y}_{\mathrm{tr}_2}\left(\tau_{\mathrm{sw}_2}\right) \\ \vdots \\ Y_{\mathrm{tr}_m}\left(\tau_{\mathrm{sw}_m}\right) \\ \dot{Y}_{\mathrm{tr}_m}\left(\tau_{\mathrm{sw}_m}\right) \end{Bmatrix}, \qquad \{\phi\}=\begin{Bmatrix} Y_{\mathrm{ss}_1}\left(\tau_{\mathrm{sw}_2}\right)-Y_{\mathrm{ss}_2}\left(\tau_{\mathrm{sw}_2}\right) \\ \dot{Y}_{\mathrm{ss}_1}\left(\tau_{\mathrm{sw}_2}\right)-\dot{Y}_{\mathrm{ss}_2}\left(\tau_{\mathrm{sw}_2}\right) \\ Y_{\mathrm{ss}_2}\left(\tau_{\mathrm{sw}_3}\right)-Y_{\mathrm{ss}_3}\left(\tau_{\mathrm{sw}_3}\right) \\ \dot{Y}_{\mathrm{ss}_2}\left(\tau_{\mathrm{sw}_3}\right)-\dot{Y}_{\mathrm{ss}_3}\left(\tau_{\mathrm{sw}_3}\right) \\ \vdots \\ Y_{\mathrm{ss}_m}\left(\tau_{\mathrm{sw}_1}\right)-Y_{\mathrm{ss}_1}\left(\tau_{\mathrm{sw}_1}\right) \\ \dot{Y}_{\mathrm{ss}_m}\left(\tau_{\mathrm{sw}_1}\right)-\dot{Y}_{\mathrm{ss}_1}\left(\tau_{\mathrm{sw}_1}\right) \end{Bmatrix} \tag{7.19}$$

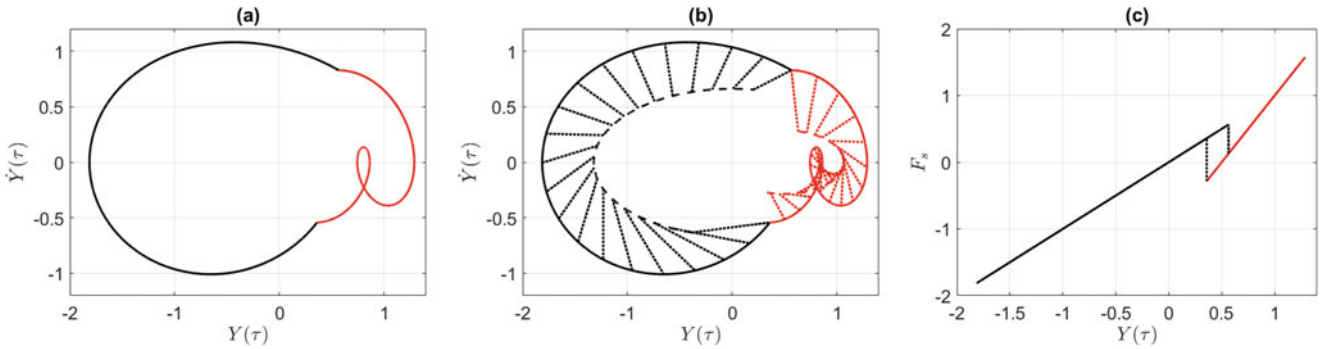

Fig. 7.1 System response of the hybrid SDOF system composed of two linear systems. (**a**) The phase plane plot of total displacement against total velocity. (**b**) The same phase plane plot with the steady-state and transient responses superimposed. (**c**) The spring force versus displacement for the two linear systems with the dotted lines showing the switch discontinuities. In all three plots, the black lines show the response when linear system 1 is active and the red lines show the response when linear system 2 is active

The transient displacements and velocities required at each switch point to ensure a periodic response may then be calculated using $\{T\} = [\lambda]^{-1}\{\phi\}$. Once the time switch transient displacements and velocities have been calculated, the values of the transient parameters A_j and B_j may then be calculated, followed by the segment responses. Note that it would have been no more complicated to formulate an expression to directly calculate the transient parameters A_j and B_j but it was felt that the current formulation would be more consistent with any future plans to extend the approach for multi-degree-of-freedom (MDOF) hybrid systems.

A numerical example will now be given to illustrate the previous theory. A hybrid system composed of two linear systems will be considered. The first linear system parameters are $\zeta_1 = 0.1$, $\gamma_1 = 1$, and $Y_{\text{offset}_1} = \dot{Y}_{\text{offset}_1} = 0$, while the second linear system parameters are $\zeta_2 = 0.1$, $\gamma_2 = 2$, $\dot{Y}_{\text{offset}_2} = 0$, and $Y_{\text{offset}_2} = 0.5$. It may be observed that the two linear systems only differ in their spring force versus displacement relationships, which are shown above in Fig. 7.1c. The forcing frequency ratio is $\alpha = 0.5$ meaning that the repeat period will be $\tau_{\text{period}} = 4\pi$. The active system vector S is [1 2] and the time switch vector will initially be set as $\tau_{\text{sw}} = [4\ 10]$. This means that linear system 1 will become active at $\tau = 4$ and remain so until $\tau = 10$, at which point linear system 2 will become active. Linear system 2 will remain active until $\tau = 4$ in the next forcing cycle and so on. Using Eqs. (7.8) and (7.9) gives a $\Delta\tau$ vector (time spent in each active system segment) as $\Delta\tau = [6\ 6.57]$. Note that these two time values sum to give the τ_{period} value. The 4×4 $[\lambda]$ matrix and the 4×1 $\{\phi\}$ column vector can then be constructed and substituted into Eqs. (7.17) and (7.19) to give the 4×1 $\{T\}$ column vector that will result in a periodic response. The various steady-state, transient, and total displacement and velocity response segments may then be calculated. These are plotted in Fig. 7.1 in the form of two phase planes and a spring force versus displacement plot. The phase plane in Fig. 7.1a shows the phase plane segments of the linear system 1 total response as a black trajectory line and the phase plane segments of the linear system 2 total response as a red trajectory line and the continuity between the two segments is clear to see. Figure 7.1b shows the same phase plane plot but with the inclusion of both the steady-state and transient phase plane segments. The dashed black and red lines show the steady-state phase plane segments of linear system 1 and linear system 2, respectively, and may be seen to take the form of elliptical arcs. Emanating from the steady-state arcs and terminating at the solid total response segments are shown a series of dotted lines that depict the progression of the transient response segments. While this plot may appear a little more cluttered than the top left plot, it does contain valuable information about how the total periodic response arises from the equilibrium between the steady-state and transient components. Figure 7.1c shows the spring force versus displacement plot for the two active systems. The discontinuities of spring force at the switches are shown by the dotted vertical lines – in the next section, an approach for eliminating these discontinuities, thereby resulting in prediction of periodic responses of piecewise linear systems, will be discussed.

7.3 Periodic Response of Harmonically-Excited Piecewise Linear Systems

The previous section presented a relatively straightforward methodology for calculating the periodic response of a harmonically excited hybrid system composed of a number of linear systems assuming that all of the switches between systems were conducted on the basis of time and were fully specified. While there may be situations, particularly in control systems, where switches are conducted on the basis of time, it will be much more common for switches between linear

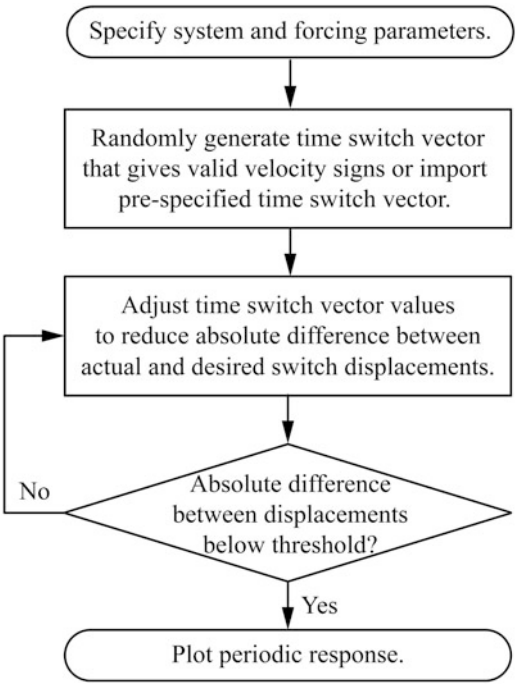

Fig. 7.2 Flowchart illustrating the iterative optimization approach for identifying the time switches to give the desired displacement switch behavior

systems to occur on the basis of displacement and/or velocity. This section will be concerned with how the time-switching method of the previous section may be exploited to predict the periodic responses of piecewise linear systems whose system parameters change on the basis of displacement. All of the ideas that are introduced here will be easily extendable to hybrid systems whose system parameters change on the basis of velocity or a combination of displacement and velocity.

For hybrid systems that require only two time switches (such as that shown in the previous section), it will be possible to conduct an exhaustive search to identify the correct time switch values to give the desired displacement switch values. For situations where there are more than two time switches, it will be preferable to adopt an iterative approach to finding the correct time switch values. This iterative approach is best described using the flowchart of Fig. 7.2. As may be seen from the flowchart, the process begins with the specification of the system parameters for each linear system and the specification of the forcing frequency ratio α. The active system vector S must also be specified to state the order in which the systems will become active – this will also specify the number of switches m. The next step of the process is to generate, or specify, a valid initial time switch vector. This may be done via the specification of an initial time switch vector that is believed to be in close proximity to the required time switch vector – this approach will be used later to calculate periodic responses over a range of frequencies. For situations where a nearby initial time switch vector cannot be specified, a randomly generated initial time switch vector may be used. It has been found that the overall method is more computationally efficient if the random generation process is repeated until the generation of an initial time switch vector that results in the desired signs for each of the velocities at the switch points. The iterative part of the process is simply updating the time switch vector values so as to reduce the difference between the desired and actual switch displacements. The size of the time switch increments will depend upon the values of the displacement differences. This process is repeated until the sum of the absolute displacement differences is less than some pre-specified threshold level, at which point the overall periodic response may be plotted.

The iterative process described above will now be employed to demonstrate how the steady-state and transient components combine to produce the overall system response for a trilinear system as the forcing frequency ratio changes. The first linear system parameters are $\zeta_1 = 0.1$, $\gamma_1 = 2$, $Y_{\text{offset}_1} = -0.5$, and $\dot{Y}_{\text{offset}_1} = 0$, the second linear system parameters are $\zeta_2 = 0.1$, $\gamma_2 = 1$, and $Y_{\text{offset}_2} = \dot{Y}_{\text{offset}_2} = 0$, and the third linear system parameters are $\zeta_3 = 0.1$, $\gamma_3 = 2$, $Y_{\text{offset}_3} = 0.5$, and $\dot{Y}_{\text{offset}_3} = 0$. This hybrid system would be a trilinear stiffness oscillator if the switches between linear system 1 and linear system 2 occurred when the displacement $Y = -1$ and the switches between linear system 2 and linear system 3 occurred when the displacement $Y = 1$. Forcing frequency ratios from $\alpha = 0.2$ to $\alpha = 1.2$ in steps of 0.2 were investigated. The active system vector S is [1 2 3 2]. The resulting phase plane plots are shown in Fig. 7.3. The solid lines again show the overall phase plane with the following colors being used: black for segment 1 (linear system 1 active), red for segment 2 (linear system 2 active for the first time), green for segment 3 (linear system 3 active), and blue for segment 4 (linear system 2 active for the second time). The dashed lines show the steady-state response segments for when each system is active and the dotted lines show the transient response segments for the same period. These plots hopefully show how the interaction between the

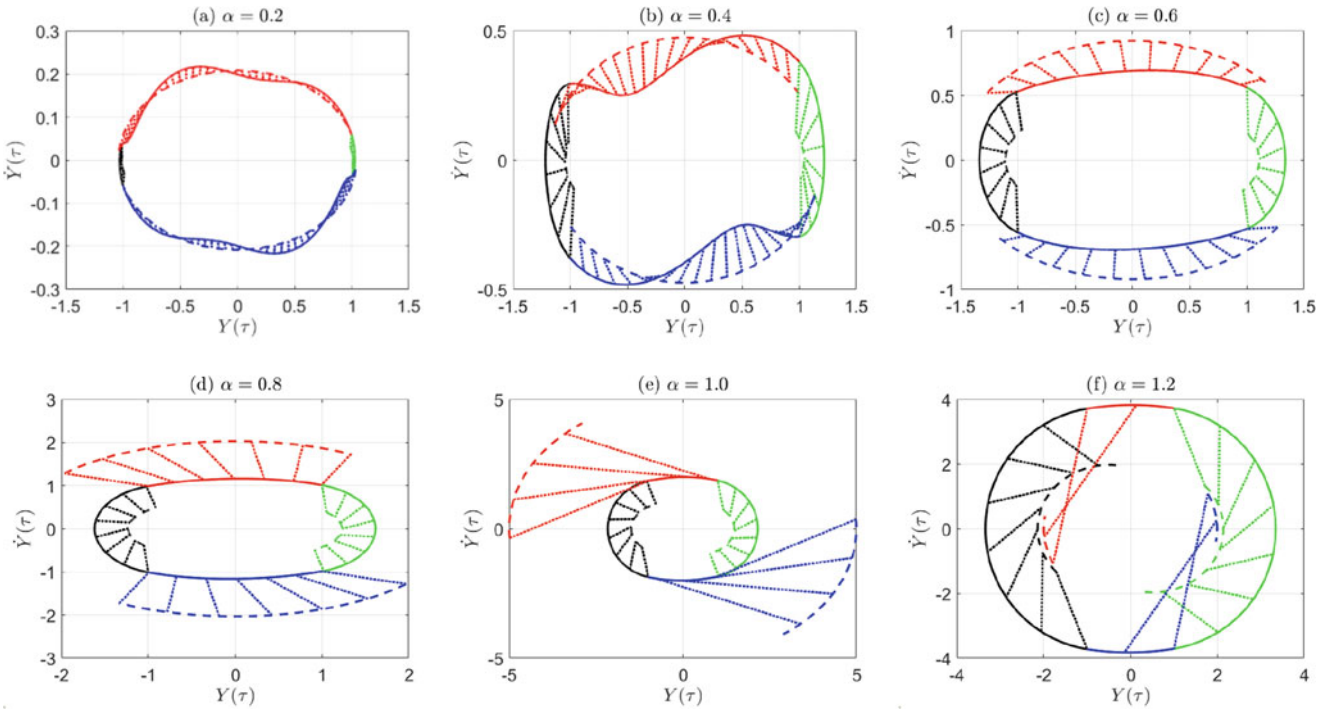

Fig. 7.3 System response of a trilinear system for various forcing frequency ratios. In all plots, the black lines show the response during segment 1, the red lines show the segment 2 response, the green lines show the segment 3 response, and the blue lines show the segment 4 response. Solid lines denote the phase plane of the overall response, while dashed lines show the steady-state components of the response when each system is active. The dotted lines emanating from the steady-state arcs show the progression of the transient components of the response

steady-state and transient responses results in the overall response. This explains how the distorted phase planes for $\alpha = 0.2$ and $\alpha = 0.4$ arise and also how the steady-state phase mismatch at $\alpha = 1.2$ results in large transient responses and a large overall response. Note that it is not possible for the trilinear system to maintain a nonlinear periodic response for $\alpha \geq 1.4$ with the only possible periodic response being the steady-state response of linear system 2.

In the previous example, there was only one possible periodic response for all forcing frequency ratios – this response was nonlinear for $\alpha < 1.4$ and linear for $\alpha \geq 1.4$. It will now be shown that, by increasing the values of the linear stiffness terms, the iterative method can identify a stable nonlinear periodic response, an unstable nonlinear periodic response in addition to the linear periodic response for a region of frequency ratios $\alpha \geq 1.4$. The stiffness parameters for linear system 1 and 3 will now be increased in value, with linear system 2 remaining the same as in the previous example. The first linear system parameters are now $\zeta_1 = 0.1$, $\gamma_1 = 5$, $Y_{\text{offset}_1} = -0.8$, and $\dot{Y}_{\text{offset}_1} = 0$; the second linear system parameters are still $\zeta_2 = 0.1$, $\gamma_2 = 1$, and $Y_{\text{offset}_2} = \dot{Y}_{\text{offset}_2} = 0$; and the third linear system parameters are $\zeta_3 = 0.1$, $\gamma_3 = 5$, $Y_{\text{offset}_3} = 0.8$, and $\dot{Y}_{\text{offset}_3} = 0$. Again, this hybrid system would be a trilinear stiffness oscillator if the switches between linear system 1 and linear system 2 occurred when the displacement $Y = -1$ and the switches between linear system 2 and linear system 3 occurred when the displacement $Y = 1$. The active system vector S is again [1 2 3 2]. The same iterative process described above was employed to identify the stable and unstable nonlinear periodic responses along with the stable linear periodic response for the region between $1.4 \leq \alpha \leq 1.8$. The process for consistently maintaining the stable or unstable nonlinear branch was through "seeding" the approach with the previous time switch vector. The active system vector S is [1 2 3 2]. The resulting phase plane plots for forcing frequency ratios from $\alpha = 1.4$ to $\alpha = 1.8$ in steps of 0.1 are shown in Fig. 7.4. On this occasion, the black lines depict the stable nonlinear response, the green lines depict the stable linear response and the red lines depict the unstable nonlinear response. The progression of the red unstable nonlinear response from being very near to the green linear response at $\alpha = 1.4$ to being very near to the black stable nonlinear response at $\alpha = 1.8$ may be clearly observed. Note that it is not possible for this trilinear system to maintain a nonlinear periodic response for $\alpha \geq 1.8$ with the only possible periodic response being the steady-state response of linear system 2.

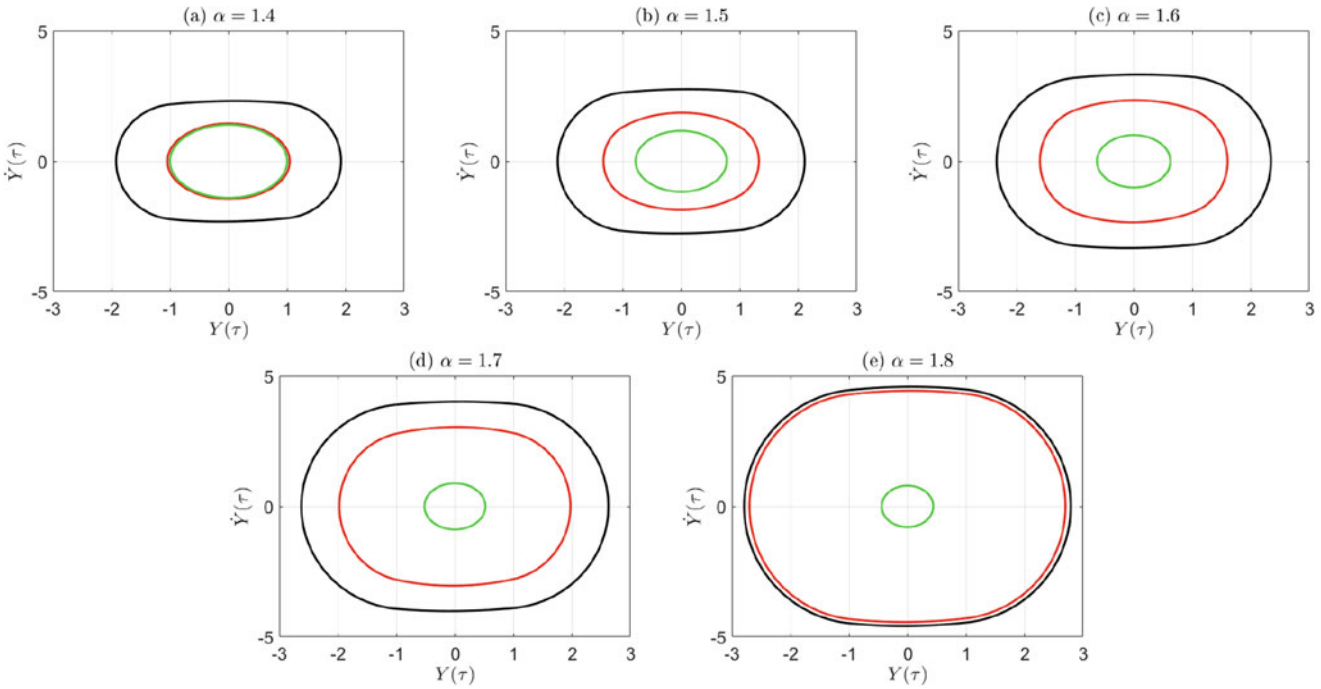

Fig. 7.4 System response of a trilinear system for various forcing frequency ratios. In all plots, the black lines show the nonlinear stable response, the red lines show the nonlinear unstable response, while the green lines show the linear stable response

7.4 Discussion and Conclusion

This chapter has presented a closed-form solution for the periodic response of a time-switched hybrid system. As stated earlier, this may be of use in some control engineering applications but the main thrust of this chapter was how this closed-form solution could be wrapped into an efficient iterative approach for the calculation of periodic responses of piecewise linear systems, including the prediction of stable and unstable solutions in the jump frequency range. The method shown can very easily be extended to other piecewise linear systems – this could include systems whereby nonlinear damping (e.g., combinations of friction and viscous damping) is represented via a number of linear systems.

That said, the true potential of this work, in the author's view, will be its possibility to be extended to continuous nonlinear systems, such as the Duffing oscillator. It is a simple matter to include more linear systems into the piecewise linear model and thereby start to approach the Duffing oscillator's stiffness curve. It is hoped that, by considering the overall response as the combination of linear steady-state and linear transient components, the ever-surprising Duffing oscillator may reveal all of its secrets.

Acknowledgments The author would like to acknowledge all the useful discussions with Professor Keith Worden regarding many things nonlinear, both in the past 25 or so years and in the last few years, since the inception of this work.

References

1. Worden, K., Tomlinson, G.: Nonlinearity in Structural Dynamics: Detection, Identification and Modelling. IoP Publishing, Bristol and Philidelphia (2001)
2. Maas, S.: Nonlinear Microwave and RF Circuits, 2nd edn. Artech House (2003)
3. Peters, J.: A beginner's guide to the Hilbert transform. Int. J. Math. Educ. Sci. Technol. **1**, 89–106 (1995)
4. Chen, S., Billings, S.: Representation of non-linear systems: the NARMAX model. Int. J. Control. **49**, 1013–1032 (1989)
5. Masri, S., Caughey, T.: A nonparametric identification technique for nonlinear dynamical problems. J. Appl. Mech. **46**, 433–447 (1979)
6. Mohammad, K., Worden, K., Tomlinson, G.: Direct parameter estimation for linear and nonlinear structures. J. Sound Vib. **152**, 471–499 (1991)
7. Volterra, V.: Theory of Functionals and Integral Equations. Dover, New York (1959)
8. Nayfeh, A.: Perturbation Methods. Wiley, New York (1973)

9. Nayfeh, A., Mook, D.: Nonlinear Oscillations. Wiley, New York (1979)
10. Vakakis, A., Manevitch, L., Mikhlin, Y., Pilipchuk, V., Zevin, A.: Normal Modes and Localization in Nonlinear Systems. Wiley-Interscience, New York (1996)
11. Kovacic, I., Brennan, M.: The Duffing Equation: Nonlinear Oscillators and their Behaviour. Wiley-Blackwell (2011)
12. Xie, L., Zhou, Y., Zhao, Y.: Criterion of chaos for switched linear systems with controllers. Int. J. Bifurcation Chaos. **20**, 4103–4109 (2010)
13. El Guezar, F., Bouzahir, H.: Chaotic behavior in a switched dynamical system. Model. Simul. Eng. **2008**, 798395 (2008)
14. Lu, J., Zhou, T., Chen, G., Yang, X.: Generating chaos with a switching piecewise-linear controller. Chaos. **12**, 344–349 (2002)